

Conductivity of disordered 2d binodal Dirac electron gas: Effect of the internode scattering

Andreas Sinner and Klaus Ziegler
Institut für Physik, Universität Augsburg
D-86135 Augsburg, Germany
(Dated: August 4, 2016)

We study the dc conductivity of a weakly disordered 2d Dirac electron gas with two bands and two spectral nodes, employing a field theoretical version of the Kubo–Greenwood conductivity formula. In this paper we are concerned with the question how the internode scattering affects the conductivity. We use and compare two established techniques for treating the disorder scattering: The perturbation theory, there ladder and maximally crossed diagrams are summed up, and the functional integral approach. Both turn out to be entirely equivalent. For a large number of random potential configurations we have found only two different conductivity scenarios. Both scenarios appear independently of whether the disorder does or does not create the internode scattering. In particular we do not confirm the conjecture that the internode scattering tends to Anderson localization.

PACS numbers: 05.60.Gg, 66.30.Fq, 05.40.-a

I. INTRODUCTION

Transport in two-dimensional (2d) electronic systems has been a subject of intense research for several decades. One of the reasons for the attractiveness of this field is that quantum interference is strong in 2d and interesting phenomena emerge, such as the quantum Hall effect. Despite of its long history, some aspects of electronic transport are still puzzling. For some time there was a consensus about the role disorder plays in transport processes, dominated by Anderson localization of electronic wave functions for conventional 2d systems [1–4]. A first hint, though, for an unconventional behavior was the transition between Hall plateaux in quantum Hall systems, which indicated the existence of a metallic state in a 2d electronic system under special conditions [5]. Even more important was the discovery of metallic states in graphene [6–8] and in a number of chemical compounds, which are commonly referred to as topological insulators [9–12], where the band structure has nodes and the electronic dispersion is linear in the vicinity of these nodes. Although these compounds represent pristine 2d systems, they reveal a finite dc conductivity which is very robust against thermal fluctuations and disorder. In the course of subsequent years these systems underwent careful studies from both the experimental and the theoretical point of view which clearly indicate that the finite dc value is a robust property.

The theoretical approach to the dc conductivity of disordered electron gases represents a notoriously difficult problem. The presence of disorder breaks explicitly the translational invariance, which obscures most of the tools of pristine microscopic analysis. An alternative way follows via the restoration of the translational invariance by averaging the observable quantity of interest over all disorder configuration. In practice though, the averaging of that sort can only be performed under assumption of a weak disorder, which guarantees for a well formed saddle-like shape of the free energy functional. Consequently, the calculations can be performed either in the Hamiltonian framework, which implies a partial summation of perturbative series in powers of random potential [2–4, 13–22], or in Lagrangian framework, where the structure of elementary excitations around the saddle point in a functional integral and the related field theoretical non-linear sigma models become the main object of studies [23–31]. In the course of several years both approaches developed themselves into independent branches of physics and are seldom compared directly with each other. Besides a detailed analysis of the transport properties of systems with a nodal spectrum, the comparison of different approximative approaches is a central goal in this paper.

This paper aims at the understanding of the effects of different scattering types in systems with a nodal electronic spectrum at chemical neutrality. Previous studies are inconclusive on the role intra- and internode scattering processes may play in electronic transport, ranging from essentially no difference [13] to strong statements about a localization–antilocalization transition [14–16], while general symmetry arguments indicate that massless modes should survive in the presence of random internode scattering [32, 33].

We pursue a two-stage program, starting with the discussion of the averaging procedure based on the combination of functional integrals for quasiparticles with different statistics. This leads us to an effective field theory in terms of graded matrix fields. The nontrivial vacuum of this theory turns out to be identical with the self-consistent Born approximation which is employed in the later parts of the paper. The inverse propagator of the effective action, obtained as Gaussian fluctuations around this vacuum, turns out to be identical, up to a unitary transformation, with the solutions of the Bethe–Salpeter equation. In the second part of the program we develop further the weak scattering formalism, formulated in our recent papers [32–38]. Besides the already mentioned comparison of two approaches, we calculate the conductivity for 16 different disorder types. We detect two apparently different conductivity scenarios, which we call Type I and II scenario. The conductivity in first scenario arises solely from the channel of ladder diagrams (LC-channel), which includes all diagrams without intersecting impurity lines, while the contribution from the channel of maximally crossed diagrams (MC-channel) is zero. In the second case, the MC-channel gives rise to the conductivity, while the contribution from the LC-channel is zero. Nonetheless, the evaluation of the Bethe–Salpeter equation with the self-consistent evaluation of the scattering rate reveals the presence of massless modes in both channels for nearly all disorder types but with different degeneracy. This indicates that not all massless modes contribute to the Kubo–Greenwood formula. Our analysis does not confirm the widespread perception that the discrete symmetries of the Hamiltonian determines uniquely the transport properties. In particular we do not observe any unique correlations between the Cartan class of a particular random Hamiltonian with its dc conductivity calculated from the Kubo–Greenwood formula. This is in line with previous observations [47,48].

The scope of this paper is as follows: In Section II we introduce the effective model which is studied subsequently. Apart from the tight-binding approximation for non-interacting electrons on a 2d bipartite lattice, which yields a degenerated linear Dirac spectrum in the low-energy domain, we discuss the phenomenology of different types of scattering in a random potential landscape. Furthermore we introduce and explain the conductivity Kubo–Greenwood formula based on the density–density correlation function [27,34–40], which is evaluated in the course of this work. The link between this version of the Kubo–Greenwood formula and diffusion is briefly discussed in Appendix A. In Section III we study the Gaussian fluctuations of the model within a functional integral approach, based on the notion of an intrinsic graded symmetry of the two-particle Green’s function. Some technical details are moved into Appendices B and C. We continue in Section IV and in Appendix D, where we approach the conductivity of the model by employing the perturbative averaging technique. We obtain generic expressions for the conductivity regardless of the disorder type and evaluate it for 16 different types in Section V.

II. MODEL

The dynamics of free electrons on bipartite lattices is governed by the family of tight-binding Hamiltonians

$$H_0 = -t \sum_{\langle rr' \rangle} (c_r^\dagger d_{r'} + d_r^\dagger c_{r'}) , \quad (1)$$

where c and d (c^\dagger and d^\dagger) are the fermionic annihilation (creation) operators with respect to each sublattice of a bipartite lattice, respectively. The neighboring lattice sites r and r' are connected with the hopping amplitude t , and the summation is performed over nearest neighbor pairs only. Although we ultimately consider the case of the honeycomb lattice with the Fermi energy laying at the nodal points, the analysis is valid for other types of bipartite lattices as well. The Hamiltonian is readily diagonalized by Fourier transformation and yields on a honeycomb lattice a well-known spectrum with two nodes. As a striking feature, close to these nodes the fermion dispersion is linear and therefore describes massless Dirac particles [41,42]. In order for the Hamiltonian to remain invariant under the time-reversal transformation both Dirac cones must be linked to each other by a parity transformation, i.e. they have different chiralities. Sometimes, the gas of such electrons at chemical neutrality is called the Weyl semimetal [43]. The effective low-energy Hamiltonian accounts for both Dirac species and reads [41,42]

$$H_0 \simeq v_F \begin{pmatrix} p_1 \sigma_1 + p_2 \sigma_2 & 0 \\ 0 & p_1 \sigma_1 - p_2 \sigma_2 \end{pmatrix} \equiv v_F \begin{pmatrix} h & 0 \\ 0 & \sigma_3 h^T \sigma_3 \end{pmatrix} = v_F (p_1 \Sigma_{01} + p_2 \Sigma_{32}) , \quad (2)$$

where matrices $\Sigma_{ij} = \sigma_i \otimes \sigma_j$, $\sigma_{i,j}$ are the unity ($i, j = 0$) and 3 Pauli ($i, j = 1, 2, 3$) matrices in the usual representation, the momentum operators are $p_i = -i\hbar\nabla_i$, v_F denoting the Fermi velocity. Below we use dimensionless energy units, i.e. $\hbar v_F = 1$ in units of inverse length.

Disorder appears in the model in form of one-particle random potentials V which are matrices in the Dirac space. Due to the mentioned nodal degeneracy in the electronic spectrum, all possible disorder scattering processes can be roughly subdivided into those with and without mixing of electrons with different chiralities. The former processes are referred to as the intranode scattering. Corresponding random low-energy Hamiltonians have the diagonal block structure

$$H = \begin{pmatrix} h + V_+ & 0 \\ 0 & \sigma_3 h^T \sigma_3 + V_- \end{pmatrix}, \quad (3)$$

where V_{\pm} denotes the random part, i.e. each block can be diagonalized independently. On the other hand, electrons whose scattering involves a change of the chirality are referred to as internode scattering processes. Corresponding Hamiltonians have the following generic form

$$H = \begin{pmatrix} h_+ & V \\ V^* & \sigma_3 h_+^T \sigma_3 \end{pmatrix}. \quad (4)$$

The Hamiltonian can also be written as $H = H_0 + V$ with the 4×4 random matrix

$$V = v_{ij} \Sigma_{ij}, \quad (5)$$

where v_{ij} is the random coordinate-dependent part and the summation convention is used. Then, the decomposition coefficients with $i = 0, 3$ are those responsible for the intra-node scattering, while $i = 1, 2$ is for inter-node scattering. In this paper we concentrate on a somewhat simpler model, where each disorder type has a decomposition with one term only; i.e.,

$$V = v \Sigma_{ij}, \quad i, j \text{ fixed}. \quad (6)$$

In a usual fashion we assume for the random part of the disorder potential a Gaussian distribution independently for each site with

$$\langle v(r) \rangle_g = 0, \quad \langle v(r) v(r') \rangle_g = g \delta(r - r'), \quad (7)$$

where g is referred to as the disorder strength and $\langle \dots \rangle_g$ denotes the ensemble averaging. Then the disorder strength is measured in units of $(\hbar v_F)^2$ and the quantity $s = (\hbar v_F)^2$ represents an appropriate reference scale.

Special cases: The case $V_+ = -V_- = \mu \sigma_0$ (i.e., for Σ_{30} disorder) is equivalent (up to an orthogonal transformation) to a single Dirac with random scalar potential [39]. Moreover, the case of Σ_{03} is related to the random gap model [30]. The latter has only one massless mode, corresponding to a massless fermion mode in the functional integral [26] or to a maximally crossed diagram in the weak perturbation series [32].

A. The Kubo–Greenwood conductivity formula

Motivated by the phenomenon of diffusion at large times [24,31,44] (cf. Appendix A), we consider the field theoretical version of the Kubo–Greenwood conductivity formula

$$\bar{\sigma}_{\mu\mu} = \frac{e^2}{h} \lim_{\epsilon \rightarrow 0} \int dE \Gamma_{\mu}(E, \epsilon) \frac{f(E) - f(E + i\epsilon)}{i\epsilon}, \quad (8)$$

where $f(E)$ is the Fermi function, ϵ is the zero-temperature Matsubara frequency, and the disorder averaged core function reads

$$\Gamma_{\mu}(E, \epsilon) = \epsilon^2 \text{Tr}_d \sum_r r_{\mu}^2 \langle G^+(r, 0) G^-(0, r) \rangle_g, \quad (9)$$

where $G^+(r, r')$ ($G^-(r, r')$) denotes the microscopic advanced (retarded) single-particle Green's function at energy E analytically continued into the upper (lower) halfplane

$$G^\pm(r, r') = \langle r | [E \pm i\epsilon + H_0 + V]^{-1} | r' \rangle. \quad (10)$$

The operator Tr_d denotes the trace operator on the space of d -dimensional Green's functions. At frequencies small as compared to the typical band width of the clean system and well below room temperature we can employ the usual approximation $f(E + i\epsilon) \sim f(E) + i\epsilon\delta(E)$, which trivializes the energy integral in Eq. (8). Then the conductivity formula becomes

$$\bar{\sigma}_{\mu\mu} = \lim_{\epsilon \rightarrow 0} \epsilon^2 \left(-\frac{\partial^2}{\partial q_\mu^2} \right) \Big|_{q=0} \sum_r e^{iq \cdot r} \langle G_{ij}^+(r, 0) G_{ji}^-(0, r) \rangle_g, \quad (11)$$

where we have used the Fourier representation of the position operator and the summation convention for matrix elements with respect to the spinor index. Due to the randomness each realization of the system lacks translational invariance and the Green's function depends on both sites r and r' . The establishing of the translational invariance is achieved by the averaging procedure. In Sections III and IV we demonstrate how the averaging is performed within a functional-integral formalism and a diagrammatic weak-scattering formalism, respectively.

III. FUNCTIONAL INTEGRAL APPROACH

The functional integral approach to disorder averaged quantities and eventually to the conductivity can be based on a functional integral with a fermionic and a bosonic field. Usually the propagators for both fields are identical, and the functional integral is called supersymmetric [21]. An alternative to this supersymmetric functional integral is based on the identity between the determinants of two different Green's functions [26,30,31]

$$\det G = \det G'. \quad (12)$$

Then we can use the Green's function G for the fermionic field and G' for the bosonic field (or vice versa) and calculate the average product $\langle GG' \rangle$ within this functional-integral representation. In our specific case we have the determinant identity (cf. Appendix B)

$$\det[i\epsilon + H_0 + V] = \det[i\epsilon + H_0^T - \mathcal{O}V\mathcal{O}], \quad (13)$$

where H_0^T describes the Hamiltonian transposed on all spaces and the operator \mathcal{O} satisfies the condition

$$H_0 = -\mathcal{O}H_0^T\mathcal{O}. \quad (14)$$

For the Dirac Hamiltonian it is important to notice the transposition rule of the momentum operator: $p_i^T = -p_i$, due to the property of the differential operator $\partial_{x_i}^T = \partial_{-x_i} = -\partial_{x_i}$. Therefore with $H_0 = p_1\Sigma_{01} + p_2\Sigma_{32}$ follows $H_0^T = -p_1\Sigma_{01} + p_2\Sigma_{32}$ and either $\mathcal{O} = \Sigma_{01}$ or $\mathcal{O} = \Sigma_{31}$. The identity (13) is valid for the Dirac Hamiltonian in Eq. (2) and for any random potential $V = v\Sigma_{ij}$ obeying $\text{Tr}_d V = 0$. The latter condition rules out the totally degenerated random potential $V = v\Sigma_{00}$, which is discussed separately in Appendix C.

The identity (13) allows us to write the disorder averaged of two-particle Green's function in Eq. (27)

$$\begin{aligned} K_{rr'} &= \text{Tr}_d \langle [i\epsilon + H_0 + V]_{rr'}^{-1} [-i\epsilon + H_0 + V]_{r'r}^{-1} \rangle_g \\ &= -\text{Tr}_d \langle [i\epsilon + H_0 + V]_{rr'}^{-1} \mathcal{O} [i\epsilon + H_0^T - \mathcal{O}V\mathcal{O}]_{r'r}^{-1} \mathcal{O} \rangle_g \\ &= \mathcal{O}_{jk} \mathcal{O}_{li} \langle \chi_{r,kj} \bar{\chi}_{r',il} \rangle_{\hat{Q}}. \end{aligned} \quad (15)$$

For the last equation we have used a functional integral with respect to the matrix field

$$\hat{Q} = \begin{pmatrix} Q & \chi \\ \bar{\chi} & iP \end{pmatrix}. \quad (16)$$

The 4×4 matrices Q, P with commuting elements, and $\bar{\chi}, \chi$ with anticommuting elements are hermitian, and thus can be expanded in a basis which includes a four-dimensional unity matrix and 15 traceless matrices, which are fifteen Γ -matrices. The functional integral is defined as

$$\langle \cdots \rangle_{\hat{Q}} = \int \cdots e^{-\mathcal{S}_G} \prod_r d\bar{\chi}_r d\chi_r dQ_r dP_r \quad (17)$$

with the action \mathcal{S}_G

$$\mathcal{S}_G[\hat{Q}] = \frac{1}{2} \text{Trg} \int d^2r d^2r' \left\{ \frac{1}{g} \delta_{rr'} \hat{Q}_r \hat{Q}_{r'} - \hat{G}(r, r') \hat{Q}_{r'} \hat{\Sigma} \hat{G}(r', r) \hat{Q}_r \hat{\Sigma} \right\} \quad (18)$$

and with frequency- and position-dependent Green's functions

$$\hat{G}(r, r') = \langle r | [iz + \hat{H}_0]^{-1} | r' \rangle, \quad (19)$$

where $\hat{H}_0 = \text{diag}[H_0, H_0^T]$, $H_0 = p_1 \Sigma_{01} + p_2 \Sigma_{32}$, and $z = \epsilon + \eta$. The operator Trg denotes the graded trace with $\text{Trg} \hat{Q} = \text{Tr} Q - i \text{Tr} P$. Eq. (18) is the result of the saddle-point approximation of a more complex functional integral, taking only fluctuations up to quadratic (Gaussian) order into account. The saddle point equation reads

$$\frac{i\eta}{g} = - \int \frac{d^2q}{(2\pi)^2} [iz + \hat{H}_0]^{-1} = \int \frac{d^2q}{(2\pi)^2} \frac{iz}{z^2 + q^2}. \quad (20)$$

The action in Eq. (18) can be decomposed into bosonic and fermionic sectors: $\mathcal{S}_G = \mathcal{S}[Q] + \mathcal{S}[P] + \mathcal{S}[\bar{\chi}, \chi]$. Expanding the kernel of the bilinear expression in powers of the momentum of the field (equivalent to a gradient expansion in real space), we obtain at zeroth order

$$\mathcal{S}[Q] = \frac{1}{2g} \int \frac{d^2q}{(2\pi)^2} Q_{ab}(q) M_{a\alpha, b\beta}^Q Q_{\alpha\beta}(-q), \quad (21)$$

$$\mathcal{S}[P] = \frac{1}{2g} \int \frac{d^2q}{(2\pi)^2} P_{ab}(q) M_{a\alpha, b\beta}^P P_{\alpha\beta}(-q), \quad (22)$$

$$\mathcal{S}[\bar{\chi}, \chi] = \frac{1}{g} \int \frac{d^2q}{(2\pi)^2} \bar{\chi}_{ab}(q) M_{a\alpha, b\beta}^X \chi_{\alpha\beta}(-q) \quad (23)$$

with

$$M_{a\alpha, b\beta}^Q = \delta_{\alpha\beta} \delta_{ab} - g \int \frac{d^2p}{(2\pi)^2} [\Sigma_B G^-(p)]_{\beta a} [\Sigma_B G^-(p)]_{b\alpha}, \quad (24)$$

$$M_{a\alpha, b\beta}^P = \delta_{\alpha\beta} \delta_{ab} - g \int \frac{d^2p}{(2\pi)^2} [\mathcal{O} \Sigma_B G^+(p) \mathcal{O}]_{\beta a} [\mathcal{O} \Sigma_B G^+(p) \mathcal{O}]_{b\alpha}, \quad (25)$$

$$M_{a\alpha, b\beta}^X = \delta_{\alpha\beta} \delta_{ab} - g \int \frac{d^2p}{(2\pi)^2} [\Sigma_B G^-(p)]_{\beta a} [\mathcal{O} \Sigma_B G^+(p) \mathcal{O}]_{b\alpha} \quad (26)$$

with $G^\pm(p) = [\pm i\eta + H_0]^{-1}$. Note the missing combinatorial factor $1/2$ in $\mathcal{S}[\bar{\chi}, \chi]$, since it counts both permutations $\bar{\chi}\chi$ and $\chi\bar{\chi}$. Once the fluctuations in Eq. (21) – (23) are expressed as quadratic forms in terms of real valued expansion coefficients of fields $Q, P, \bar{\chi}$, and χ , the eigenvalues of the corresponding inverse propagator matrices become nonnegative.

The expansion of Eq. (18) to second order in the momenta yields the inverse (diffusion) propagators. This enables us to compare the functional-integral approach with a weak-scattering expansion of Section IV. In particular, the expression for zero momentum, which represents the mass matrices, has non-zero eigenvalues. Zero eigenvalues are most important, since they correspond to diffusion modes.

IV. PERTURBATIVE AVERAGING APPROACH TO THE CONDUCTIVITY

In the second part of our program we approach the dc conductivity within a weak scattering approach, in which the disorder average is performed perturbatively. This is the standard method in the weak-localization approach, in which the Green's functions are expanded in terms of the random scattering

elements and averaged afterwards [2–4,13–22]. As an extension of the analysis in our recent papers [32,33], where we were concerned with the conductivity behavior in the single-cone approximation, here we take both cones into account. The averaged two-particle Green's function

$$K_{rr'} = \langle G_{nj}^+(r, 0) G_{jn}^-(0, r) \rangle_g \quad (27)$$

is treated within a perturbative expansion in powers of weak scattering rate η , which plays the role of the order parameter in diffusive regime. It is determined self-consistently from

$$\pm i\eta = -\frac{1}{d} \sum_{r'} \text{Tr}_d \langle V(r) G^\pm(r, r') V(r') \rangle_g = -\frac{g}{d} \text{Tr}_d [\Sigma \bar{G}^\pm(r, r) \Sigma], \quad (28)$$

where Σ are disorder matrices in Dirac space. The averaged one-particle Green's functions become translationally invariant and read

$$\bar{G}^\pm(r, r') = \langle r | [\pm iz + H_0]^{-1} | r' \rangle = \int \frac{d^2 p}{(2\pi)^2} e^{ip(r-r')} \frac{\tilde{H}_0 \mp iz}{p^2 + z^2}, \quad (29)$$

with $z = \epsilon + \eta$ and \tilde{H}_0 denoting the Fourier-transformed Hamiltonian. \tilde{H}_0 is not rotational invariant and does not contribute to the integral. We recognize then in Eq. (28) the saddle point of the functional integral defined in Eq. (20). For $\epsilon \sim 0$ we get

$$1 - \int \frac{d^2 p}{(2\pi)^2} \frac{g}{p^2 + z^2} \sim \frac{\epsilon}{\eta}. \quad (30)$$

Partial summations of all ladder (LC) and maximally crossed (MC) diagrams (see Appendix D) lead to

$$\begin{aligned} \bar{\sigma}_{\mu\mu} &= \lim_{\epsilon \rightarrow 0} \epsilon^2 \left(-\frac{\partial^2}{\partial q_\mu^2} \right) \Big|_{q=0} \sum_{rr'} e^{iq \cdot r} \bar{G}_{ij}^+(r', 0) \bar{G}_{kn}^-(0, r') \\ &\times \left[(1 - g[\bar{G}^+ \Sigma][\bar{G}^- \Sigma])_{rr'|nj;ik}^{-1} + (1 - g[\bar{G}^+ \Sigma][\bar{G}^- \Sigma]^T)_{rr'|nk;ij}^{-1} \right], \end{aligned} \quad (31)$$

where the full transposition operator T applies to all degrees of freedom. We shall call the terms in the second line of Eq. (31)

$$a) \ t = g[\bar{G}^+ \Sigma][\bar{G}^- \Sigma], \quad b) \ \tau = g[\bar{G}^+ \Sigma][\bar{G}^- \Sigma]^T \quad (32)$$

the LC (Eq. (32a)) and the MC (Eq. (32b)) channel matrices, respectively [32]. These matrices read in Fourier representation

$$t_{r'r|ab;cd} = g \int \frac{d^2 q}{(2\pi)^2} e^{-iq \cdot (r-r')} \int \frac{d^2 p}{(2\pi)^2} [\bar{G}^+(p) \Sigma]_{ac} [\bar{G}^-(q+p) \Sigma]_{bd}, \quad (33)$$

$$\tau_{r'r|ab;cd} = g \int \frac{d^2 q}{(2\pi)^2} e^{-iq \cdot (r'-r)} \int \frac{d^2 p}{(2\pi)^2} [\bar{G}^+(p) \Sigma]_{ac} [\bar{G}^-(q-p) \Sigma]_{db}. \quad (34)$$

The different signs in the argument of t and τ are a consequence of the transposition on the position space in the MC-channel. Fourier transformed matrices $1 - \tilde{t}_q$ and $1 - \tilde{\tau}_q$ for $\epsilon = 0$ and $q = 0$ read

$$M_{ab;cd}^{LC} = \delta_{ac} \delta_{bd} - g \int \frac{d^2 p}{(2\pi)^2} [\bar{G}^+(p) \Sigma]_{ac} [\bar{G}^-(p) \Sigma]_{bd} \Big|_{\epsilon=0}, \quad (35)$$

$$M_{ab;cd}^{MC} = \delta_{ac} \delta_{bd} - g \int \frac{d^2 p}{(2\pi)^2} [\bar{G}^+(p) \Sigma]_{ac} [\bar{G}^-(-p) \Sigma]_{db} \Big|_{\epsilon=0}. \quad (36)$$

Matrices M in Eqs. (35) and (36) are diagonalized by the momentum independent orthogonal transformations O . The eigenvalues of the matrices M provide a decay length for the matrices in Eq. (32). In particular, a vanishing (e.g. gapless) eigenvalue gives a long-range diffusion-like behavior. Depending

on the type of disorder there may or may not be gapless modes. If gapless modes exist, then for small momenta and frequencies we get in the LC channel (in the channel of MC diagrams analogously)

$$t_{r'r} \sim O_{LC} \text{diag}[t]_{r'r} O_{LC}^T \sim \int \frac{d^2q}{(2\pi)^2} e^{iq \cdot (r-r')} O_{LC} \begin{bmatrix} \left(\frac{\epsilon}{\eta} + gD_0q^2\right) 1_N & \mathbf{0}^T \\ \mathbf{0} & \hat{\Lambda}_{D-N} \end{bmatrix} O_{LC}^T, \quad (37)$$

where N is the dimension of the subspace populated by gapless modes. $\hat{\Lambda}_{D-N}$ represents the diagonal matrix with non-zero eigenvalues of M^{LC} as matrix elements. D is the dimension of the full space on which the product $G^+ \otimes G^-$ dwells, and D_0 is the expansion coefficient, which fortunately turns out to be the same for all studied cases:

$$D_0 = \frac{1}{2} \int \frac{d^2p}{(2\pi)^2} \frac{1}{[p^2 + \eta^2]^2} \sim \frac{1}{8\pi\eta^2}. \quad (38)$$

Finally, $\mathbf{0}$ is an $(D - N) \times N$ matrix whose elements are zero. Using the convolution formula for the tensor product of two Green's functions

$$\bar{G}_{ij}^+(r, 0) \bar{G}_{kn}^-(0, r) = \int \frac{d^2p}{(2\pi)^2} e^{-ip \cdot r} \int \frac{d^2k}{(2\pi)^2} \bar{G}_{ij}^+(k) \bar{G}_{kn}^-(k + p), \quad (39)$$

we can bring Eq. (31) to the form where the derivatives with respect to the external momentum q can be easily evaluated. After performing the dc limit we arrive at

$$\bar{\sigma}_{\mu\mu} = 2g\eta^2 D_0 \int \frac{d^2p}{(2\pi)^2} \bar{G}_{ij}^+(p) \bar{G}_{kn}^-(p) \times \left\{ \left[O_{LC} \begin{pmatrix} 1_{N_{LC}} & \mathbf{0}^T \\ \mathbf{0} & \hat{\mathbf{0}}_{D-N_{LC}} \end{pmatrix} O_{LC}^T \right]_{nj;ik} + \left[O_{MC} \begin{pmatrix} 1_{N_{MC}} & \mathbf{0}^T \\ \mathbf{0} & \hat{\mathbf{0}}_{D-N_{MC}} \end{pmatrix} O_{MC}^T \right]_{nk;ij} \right\}, \quad (40)$$

where $\hat{\mathbf{0}}_{D-N}$ denotes a $(D - N) \times (D - N)$ zero matrix. This result indicates that the conductivity $\bar{\sigma}_{\mu\mu}$ is finite for a positive scattering rate η . In particular, it does not have a logarithmic divergence in the limit of zero temperature, as predicted in some weak localization calculations. For correct evaluation of the conductivity, the disorder strength parameter g in front of the integral must be compensated with the help of the saddle point condition (30):

$$\int \frac{d^2p}{(2\pi)^2} \bar{G}_{ij}^+(p) \bar{G}_{kn}^-(p) \Gamma_{ikjn} = \frac{1}{g} + \text{remaining terms}, \quad (41)$$

where the quantity Γ denotes the full tensor in the curly brackets. For ultimate values of the conductivity we must determine the orthogonal matrices O_{LC} and O_{MC} . This requires the explicit knowledge of the type of disorder, i.e. matrices Σ . In Section V we discuss solutions of Eq. (40) for a number of disorder types.

V. CONDUCTIVITY FOR DIFFERENT RANDOM POTENTIALS

Now we can evaluate the conductivity of a binodal Dirac electron gas in a random potential from Eq. (31). In order to investigate the role of the disorder mediated intermixing of Dirac electrons with different chiralities we use the full renormalized Dirac propagators $\bar{G}^\pm(p)$ which read in Fourier representation

$$\bar{G}^\pm(p) = \frac{1}{p^2 + \eta^2} \begin{pmatrix} \mp i\eta & p_1 - ip_2 & 0 & 0 \\ p_1 + ip_2 & \mp i\eta & 0 & 0 \\ 0 & 0 & \mp i\eta & p_1 + ip_2 \\ 0 & 0 & p_1 - ip_2 & \mp i\eta \end{pmatrix}. \quad (42)$$

Matrix Σ_{ab}	0	a	2a	2b	2(a+b)	a+2b
Σ_{00}	4	8	4	0	0	0
Σ_{01}	4	4	0	4	0	4
Σ_{02}	2	4	2	2	2	4
Σ_{30}	2	4	2	2	2	4
Σ_{31}	2	4	2	2	2	4
Σ_{32}	4	4	0	4	0	4
Σ_{10}	2	4	2	2	2	4
Σ_{11}	2	4	2	2	2	4
Σ_{13}	2	4	2	2	2	4
Σ_{20}	2	4	2	2	2	4
Σ_{21}	2	4	2	2	2	4
Σ_{23}	2	4	2	2	2	4

TABLE I: Eigenvalues and their number of the mass matrices in LC channel for the random potentials $v\Sigma_{ab}$ giving Type I conductivity.

Matrix Σ_{ab}	0	a	2a	2b	2(a+b)	a+2b
Σ_{03}	2	4	2	2	2	4
Σ_{33}	0	8	0	4	4	0
Σ_{12}	2	4	2	2	2	4
Σ_{22}	2	4	2	2	2	4

TABLE II: Eigenvalues and their number of the mass matrices in LC channel for the random potentials $v\Sigma_{ab}$ giving Type II conductivity.

Different disorder types were studied by inserting respective disorder matrices Σ_{ij} directly into Eqs. (31) and then unfolding them up to the form of Eq. (40). In all we have evaluated the conductivity for 16 different disorder configurations. Technically, the evaluation of the conductivity contributions for each disorder type does not differ much from the single-cone model evaluation presented in our recent papers Ref. [32,33]. The number of massless modes is obtained by counting zero eigenvalues of the corresponding mass matrices given in Eqs. (35) and (36). Despite high dimensionality of the matrices (16×16 or even 64×64), the order of the characteristic polynomial is small, since the matrices are sparsely occupied. In the case of 16×16 -matrices, of 256 matrix elements only 24 to 32, depending on the disorder type, are non-zero. Moreover the mass matrices are symmetric. Consequently, they can be diagonalized analytically using a computer algebra package. Then, the calculation of the conductivity from Eq. (40) can be carried out exactly. Surprisingly, for all 16 types of random matrices we have discovered only two distinct conductivity types. Both types occur for disorder potentials with and without chirality mixing and have their own features:

Type 1: Reveals a total suppression of the contribution from the MC-channel:

$$\sigma_{\mu\mu}^{MC} \sim 0. \quad (43)$$

The conductivity is entirely controlled by the LC-channel, which yields

$$\sigma_{\mu\mu}^{LC} \sim 4\eta^2 D_0 \sim \frac{1}{2\pi}. \quad (44)$$

This conductivity type was found for $\Sigma_{00}, \Sigma_{01}, \Sigma_{02}, \Sigma_{30}, \Sigma_{31}, \Sigma_{32}, \Sigma_{10}, \Sigma_{11}, \Sigma_{13}, \Sigma_{20}, \Sigma_{21}, \Sigma_{23}$.

Type 2: Demonstrates a picture somewhat reciprocal to the Type 1: The conductivity contribution from the LC-channel is fully suppressed

$$\sigma_{\mu\mu}^{LC} \sim 0, \quad (45)$$

Matrix Σ_{ab}	0	a	2a	2b	2(a+b)	a+2b
Σ_{00}	4	8	4	0	0	0
Σ_{01}	0	4	4	0	4	4
Σ_{02}	2	4	2	2	2	4
Σ_{30}	2	4	2	2	2	4
Σ_{31}	2	4	2	2	2	4
Σ_{32}	0	4	4	0	4	4
Σ_{10}	2	4	2	2	2	4
Σ_{11}	2	4	2	2	2	4
Σ_{13}	2	4	2	2	2	4
Σ_{20}	2	4	2	2	2	4
Σ_{21}	2	4	2	2	2	4
Σ_{23}	2	4	2	2	2	4

TABLE III: Eigenvalues and their number of the mass matrices in MC channel for the random potentials $v\Sigma_{ab}$ giving Type I conductivity.

Matrix Σ_{ab}	0	a	2a	2b	2(a+b)	a+2b
Σ_{03}	2	4	2	2	2	4
Σ_{33}	4	0	4	0	0	8
Σ_{12}	2	4	2	2	2	4
Σ_{22}	2	4	2	2	2	4

TABLE IV: Eigenvalues and their number of the mass matrices in MC channel for the random potentials $v\Sigma_{ab}$ giving Type II conductivity.

while the MC-channel gives

$$\sigma_{\mu\mu}^{MC} \sim 8\eta^2 D_0(1-a), \quad (46)$$

where the parameter a is defined below in Eq. (50). The Type 2 conductivity exhibits a logarithmically suppressed conductivity and was found for $\Sigma_{03}, \Sigma_{33}, \Sigma_{12}, \Sigma_{22}$.

Having found only two conductivity types, it is natural to expect that the corresponding disorder matrices share some common features. We would expect that the microscopic random Hamiltonians, which lead to the same conductivity type, belong to the same Cartan classes. This property of the random Hamiltonians is usually brought into connection with the expected Anderson localization transition in the system [45–48]. According to the Altland–Zirnbauer classification of $N \times N$ random matrices, the behavior of a random Hamiltonian under the time-reversal, particle-hole, and chiral symmetry transformations determines to which Cartan class this Hamiltonian belongs:

$$TH^*T^\dagger = H, \quad \text{Time – reversal symmetry} \quad (47)$$

$$CH^TC^\dagger = -H, \quad \text{Particle – hole symmetry} \quad (48)$$

$$PHP^\dagger = -H, \quad \text{Chiral symmetry} . \quad (49)$$

Here H^* denotes the complex conjugate of the Hamiltonian H and H^T its transposition on all spaces. If we extend the $N \times N$ random matrix ensembles by including a spatial Dirac operator, the number of classes increases at least to 17 for the single-node Dirac-like Hamiltonians [47,48] and may increase even further when two nodes and inter-node scattering is included. Therefore, the classification of random Hamiltonians given by Eq. (3) remains a great challenge. In the present work we focus only on the characterization of the transport properties. We notice that the mass matrices in both LC and MC channels are unique to each disorder matrix Σ_{ij} . The composition of the sets of eigenvalues for each disorder matrix Σ_{ij} (in particular the number of zero eigenvalues) may differ from each other, even if the

microscopic Hamiltonians formally belong to the same Cartan class. The sets of eigenvalues of the mass matrices are shown in Tables I-IV for both channels with the notation

$$a = \int \frac{d^2 p}{(2\pi)^2} \frac{gp^2}{[p^2 + \eta^2]^2}, \quad b = \int \frac{d^2 p}{(2\pi)^2} \frac{g\eta^2}{[p^2 + \eta^2]^2}. \quad (50)$$

A systematic property of the eigenvalue sets consists in the total number of zero eigenvalues per LC and MC channels together. There are always 4 with the only important exclusion of the totally degenerated disorder which couples to the unity matrix on the extended space Σ_{00} . In the latter case the number of zero eigenvalues is doubled; i.e., 8 instead of 4. This observation is linked back to the continuous symmetry on the configuration space which spontaneously breaks down in order to give rise to the gapless excitations is the same for all disorder types [31,32,39]. In the case of Σ_{00} -case the symmetry lives in a space which is twice as large, cf. Appendix C. This explains the higher number of massless modes. The order parameter in all cases is the scattering rate η .

Within the functional-integral approach we obtain the same sets of eigenvalues for the various disorder types, as summarized in Tables I-IV. A direct correspondence between the modes of LC- and MC-channel on the one hand, and the fermionic and the bosonic field on the other can be obtained for the random matrices with Σ_{01} and Σ_{32} . These cases are related to the Type 1 conductivity (cf. Tables I and II). For Σ_{33} , which is Type 2 conductivity (Tables III and IV), the full set of eigenvalues in LC-channel (with no zero eigenvalues) is reproduced in both bosonic (Q and P) channels, while the full set of eigenvalues of MC-channel arises from the fermionic channel. Thus, the full equivalency of both averaging procedures is established.

Since both conductivity types occur due to the spontaneous breaking of the same continuous symmetry, the origin of the different transport properties must be in the discrete transformations of the effective Hamiltonian on the configuration space. These symmetries are difficult to realize within the perturbative approach of Section IV but can be recognized using functional integral representation which we discussed in Section III. The generator \mathcal{T} with $\mathcal{T}\mathcal{T} = 1$ can be considered as an effective time-reversal transformation, when it distinguishes Hamiltonian H_0 and the random part V through the following properties:

$$a) H_0 = \mathcal{T}H_0^T\mathcal{T}, \quad b) V = -\mathcal{T}OV\mathcal{T}. \quad (51)$$

Eq. (51a) is solved either for $\mathcal{T} = \Sigma_{02}$ or $\mathcal{T} = \Sigma_{32}$. Combining this with the chiral symmetry condition of Eq. (14) for the full Hamiltonian we make the following general observation: If a matrix Σ_{ij} obeys both equalities

$$a) \Sigma_{ij} = \mathcal{T}\mathcal{O}\Sigma_{ij}\mathcal{O}\mathcal{T}, \quad \text{and} \quad b) \Sigma_{ij} = -\mathcal{O}\Sigma_{ij}\mathcal{O}, \quad (52)$$

for $\mathcal{O} = \Sigma_{01}$, $\mathcal{T} = \Sigma_{32}$, we have

$$\mathcal{T}(H_0^T + \mathcal{O}V\mathcal{O})\mathcal{T} = (H_0 + V). \quad (53)$$

This is valid for all matrices in V which lead to the Type 2 conductivity, (i.e., for $\Sigma_{03}, \Sigma_{33}, \Sigma_{12}, \Sigma_{22}$), which therefore all disobey Eq. (51b) while satisfying Eq. (52b). On the other hand, none of the corresponding matrices in V for the Type 1 scenario (i.e., for $\Sigma_{00}, \Sigma_{01}, \Sigma_{02}, \Sigma_{30}, \Sigma_{31}, \Sigma_{32}, \Sigma_{10}, \Sigma_{11}, \Sigma_{13}, \Sigma_{20}, \Sigma_{21}, \Sigma_{23}$) fulfill Eqs. (52) simultaneously. Thus, the relations (52) characterize Type 2 conductivity, the absence of them characterizes Type 1 conductivity.

VI. CONCLUSIONS

Despite decades of intense research several aspects of the disorder physics are still challenging. Novel low-dimensional materials defy traditional views and reveal a new and hitherto unexpected physics. The dc conductivity of 2d disordered nodal electron gases represents a striking example of that kind. Following the traditional theories it must necessarily disappear in infinite systems no matter how weak the disorder is. Yet the experimental evidence clearly speaks against this perception. Numerous attempts to reconcile those facts ultimately made the internode scattering processes responsible for localization. According to

this hypothesis, once such processes are realized in the physical systems, it must inevitably become an insulator.

In this work we performed an extensive studies of the dc conductivity of chemically neutral disordered 2d binodal Dirac or Weyl electron gas aiming at the question, how the internodal scattering affects the transport in such systems. Using the version of the Kubo–Greenwood formula based on the density–density correlation function, we compared two technically very different approaches to the disorder averaging: the perturbative weak scattering technique and the non–perturbative functional integral approaches. For a large number of disorder potentials we obtained from both approaches the same diffusion propagators, which eventually give rise to the conductivity. Our findings reveal a very simple picture of what happens in those systems. There are only two distinct conductivity types, the one which yields a universal conductivity value in infinite systems and the second which reveals a logarithmically suppressed conductivity. However, in contrast for instance to the weak–localization theory, even in the latter case Anderson localization never occurs and the system remains a conductor. The internode scattering can be definitely ruled out as the primary cause of the localization in nodal systems, since both conductivity types are observed for both inter- and intranode scattering potentials. A similar statement can also be made for the wide spread perception on the role of discrete symmetries of the microscopic Hamiltonians. While they definitely are important as we demonstrate in the present work, there is direct connection between the Cartan classification of the microscopic random Hamiltonian and the localization properties. At this stage, the true reason why the transport follows different types for different random potentials remains inconclusive.

Appendix A: Diffusion and conductivity

Starting from the transition probability

$$P_{rr'}(t) = \sum_{j,j'} \langle |\langle r, j | e^{-iHt} | r', j' \rangle|^2 \rangle_g, \quad (\text{A1})$$

with $\langle \dots \rangle_g$ denoting the disorder averaging we can calculate the diffusion coefficient as

$$D = \lim_{\epsilon \rightarrow 0} \epsilon^2 \sum_r (r_k - r'_k)^2 \int_0^\infty dt P_{rr'}(t) e^{-\epsilon t}. \quad (\text{A2})$$

With the Green's function $G(z) = (H - z)^{-1}$, we can write for the integral

$$\int_0^\infty dt P_{rr'}(t) e^{-\epsilon t} = \int dE \text{Tr}_d \{ G_{rr'}(E + i\epsilon) [G_{r'r}(E - i\epsilon) - G_{r'r}(E + i\epsilon)] \}, \quad (\text{A3})$$

where Tr_d is the trace with respect to the spinor index. Only the contribution with poles on both sides of the real axis is relevant. Then we can write

$$D = \lim_{\epsilon \rightarrow 0} \epsilon^2 \sum_r (r_k - r'_k)^2 \int dE \text{Tr}_d [G_{rr'}(E + i\epsilon) G_{r'r}(E - i\epsilon)]. \quad (\text{A4})$$

Appendix B: Proof of Eq. (13)

Our aim is to give a proof for Eq. (13)

$$\det[i\epsilon 1 + H_0 + V] = \det[i\epsilon 1 + H_0^T - \mathcal{O}V\mathcal{O}], \quad (\text{B1})$$

for $H_0^T = -\mathcal{O}H_0\mathcal{O}$, $\mathcal{O}\mathcal{O} = 1$ and $\text{Tr}_d[H_0 + V] = 0$, that is

$$H_0^T - \mathcal{O}V\mathcal{O} = -\mathcal{O}[H_0 + V]\mathcal{O} \quad (\text{B2})$$

Be λ_i and μ_i eigenvalues of matrices $i\epsilon 1 + H_0 + V$ and $i\epsilon 1 + H_0^T - \mathcal{O}V\mathcal{O}$, respectively, then Eq. (B1) is equivalent to

$$\prod_{i=1}^{2N} \lambda_i = \prod_{i=1}^{2N} \mu_i. \quad (\text{B3})$$

The eigenvalues in turn follow from the solutions of the corresponding secular equations

$$\det[(\lambda - i\epsilon)1 - H_0 - V] = 0 = \det[(\mu - i\epsilon)1 - H_0^T + \mathcal{O}V\mathcal{O}], \quad (\text{B4})$$

such that $\lambda' = \lambda - i\epsilon$ and $\mu' = \mu - i\epsilon$ represent the eigenvalues of random Hamiltonians $H_0 + V$ and $H_0^T - \mathcal{O}V\mathcal{O}$, respectively, and therefore real numbers. Then with Eq. (B2) follows

$$\det[\lambda'1 - H_0 - V] = 0 = \det[\mu'1 - H_0^T + \mathcal{O}V\mathcal{O}] = \det[\mathcal{O}(\mu'1 + H_0 + V)\mathcal{O}], \quad (\text{B5})$$

i.e.

$$\det[\lambda'1 - H_0 - V] = 0 = \det[\mu'1 + H_0 + V], \quad (\text{B6})$$

which obviously implies $\lambda'_i = -\mu'_i$. Because random Hamiltonians are traceless, the eigenvalues of d dimensional matrices always appear in bundles, each of which sums up to zero separately, e.g. in $d=2$ there are only two with opposite sing; in our case $d=4$ there are two pair with opposite sing $\lambda'_i \rightarrow \pm|\lambda'_i|$, i.e. $\mu'_i \rightarrow \mp|\lambda'_i|$. Then Eq. (B3) becomes

$$\prod_{i=1}^N (i\epsilon + |\lambda_i|)(i\epsilon - |\lambda_i|) = \prod_{i=1}^N (i\epsilon - |\lambda_i|)(i\epsilon + |\lambda_i|),$$

which obviously proofs Eq. (13).

Appendix C: Embedding of the totally degenerated random potential

In order to imbed the totally degenerated disorder which couples to the matrix Σ_{00} into the functional integral formalism of Section III we use the fact that $\langle V^{2n+1} \rangle_g = 0$ for any integer n , i.e. the sign of the random potential in the Hamiltonian does not affect the ultimate results. Then we can write the two-particles Green's function as

$$\begin{aligned} K_{rr'} &= \frac{1}{2} \text{Tr}_4 \langle [i\epsilon + H_0 + V]_{rr'}^{-1} [-i\epsilon + H_0 + V]_{r'r'}^{-1} \rangle_g + \frac{1}{2} \text{Tr}_4 \langle [i\epsilon + H_0 - V]_{rr'}^{-1} [-i\epsilon + H_0 - V]_{r'r'}^{-1} \rangle_g \\ &= \frac{1}{2} \text{Tr}_8 \left\langle \begin{bmatrix} i\epsilon + H_0 + V & 0 \\ 0 & i\epsilon + H_0 - V \end{bmatrix}_{rr'}^{-1} \begin{bmatrix} -i\epsilon + H_0 + V & 0 \\ 0 & -i\epsilon + H_0 - V \end{bmatrix}_{r'r'}^{-1} \right\rangle_g, \end{aligned} \quad (\text{C1})$$

and carry out calculations in this extended representation.

Appendix D: Dyson and Bethe-Salpeter equations in weak scattering regime

We briefly recapitulate the derivation of the disorder averaged Green's function for the case of weak scattering. To keep the notation simpler, here we use the symbol $\langle \dots \rangle$ to denote the ensemble average. We start with the expansion of the microscopic Green's function into the geometric series:

$$G = [G_0^{-1} + V]^{-1} \sim G_0 - G_0 V G_0 + G_0 V G_0 V G_0 - G_0 V G_0 V G_0 V G_0 \dots \quad (\text{D1})$$

Applying the averaging procedure in accord with Eq. (7) we may drop all terms containing odd powers of V . Then rearranging we get:

$$\begin{aligned} \langle G \rangle &= \langle G_0 + G_0 V G_0 V G_0 + G_0 V G_0 V G_0 V G_0 \dots \rangle \\ &= \langle G_0 + G_0 V G_0 V (G_0 + G_0 V G_0 V G_0 + G_0 V G_0 V G_0 V G_0 \dots) \rangle \\ &\sim G_0 + G_0 \langle V G_0 V \rangle \langle G \rangle = G_0 (1 + \langle V G_0 V \rangle \langle G \rangle), \end{aligned} \quad (\text{D2})$$

where we made use of the weak scattering conjecture. This yields the renormalization of G :

$$\langle G \rangle \sim (G_0^{-1} - \langle VG_0V \rangle)^{-1} \sim \bar{G}. \quad (\text{D3})$$

In an analogous fashion we consider the two-particle Green's function:

$$\langle G^+ G^- \rangle = \langle ([G_0^+]^{-1} + V)^{-1} ([G_0^-]^{-1} + V)^{-1} \rangle. \quad (\text{D4})$$

We expand the Green's function into the geometric series:

$$\begin{aligned} \langle G^+ G^- \rangle &= \langle (G_0^+ - G_0^+ V G_0^+ + G_0^+ V G_0^+ V G_0^+ \dots) (G_0^- - G_0^- V G_0^- + G_0^- V G_0^- V G_0^- \dots) \rangle \\ &= G_0^+ G_0^- + \langle (G_0^+ V G^+)(G_0^- V G^-) \rangle - G_0^+ G_0^- \langle V G^- \rangle - \langle G^+ V \rangle G_0^+ G_0^-. \end{aligned} \quad (\text{D5})$$

For assumed weak scattering the last two terms are of the order zero and we may retain only first two terms which allow for self-consistency

$$\langle G^+ G^- \rangle \sim G_0^+ G_0^- + \langle (G_0^+ V G^+)(G_0^- V G^-) \rangle. \quad (\text{D6})$$

Expanding it in a matrix basis and exploiting the weak scattering conjecture we furthermore have

$$\begin{aligned} \langle G_{ij}^+ G_{kl}^- \rangle &\sim G_{0,ij}^+ G_{0,kl}^- + \langle G_{0,ia}^+ V_{ab} G_{bj}^+ G_{0,k\alpha}^- V_{\alpha\beta} G_{\beta l}^- \rangle \\ &\sim G_{0,ij}^+ G_{0,kl}^- + \langle G_{0,ia}^+ V_{ab} G_{0,k\alpha}^- V_{\alpha\beta} \rangle \langle G_{bj}^+ G_{\beta l}^- \rangle, \end{aligned} \quad (\text{D7})$$

which then reversibly rewritten reads

$$G_{0,ij}^+ G_{0,kl}^- \sim \left[\delta_{ib} \delta_{k\beta} - \langle G_{0,ia}^+ V_{ab} G_{0,k\alpha}^- V_{\alpha\beta} \rangle \right] \langle G_{bj}^+ G_{\beta l}^- \rangle = \langle [1 - (G_0^+ V)(G_0^- V)] \rangle_{ik;b\beta} \langle G_{bj}^+ G_{\beta l}^- \rangle. \quad (\text{D8})$$

The expression on the left hand side is invariant under the averaging procedure, i.e. we can rewrite the last equation as follows:

$$\langle [1 - (G_0^+ V)(G_0^- V)] \rangle_{ik;b\beta} \left([1 - (G_0^+ V)(G_0^- V)]_{b\beta;nm}^{-1} G_{0,nj}^+ G_{0,ml}^- - \langle G_{bj}^+ G_{\beta l}^- \rangle \right) = 0. \quad (\text{D9})$$

Making again use of the weak scattering conjecture we obtain the Bethe-Salpeter equation

$$\langle G_{nj}^+ G_{ml}^- \rangle \sim \langle [1 - (G_0^+ V)(G_0^- V)]^{-1} \rangle_{nm;ik} G_{0,ij}^+ G_{0,kl}^- \quad (\text{D10})$$

which is the equation we have to evaluate. Expanding the disorder matrix in (D10) into the geometric series we get

$$\begin{aligned} \langle [1 - (G_0^+ V)(G_0^- V)]^{-1} \rangle_{nm;ik} &= \delta_{ni} \delta_{mk} + \langle (G_0^+ V)_{ni} (G_0^- V)_{mk} \rangle \\ &+ \langle (G_0^+ V)_{n\alpha} (G_0^- V)_{m\beta} (G_0^+ V)_{\alpha i} (G_0^- V)_{\beta k} \rangle + \dots \end{aligned} \quad (\text{D11})$$

Then performing the average in accord with Eq. (7) by means of the Wick theorem we get

$$\begin{aligned} \langle [1 - (G_0^+ V)(G_0^- V)]^{-1} \rangle_{nm;ik} &\sim \delta_{ni} \delta_{mk} + g (G_0^+ \Sigma)_{ni} (G_0^- \Sigma)_{mk} + \\ &+ g^2 [(G_0^+ \Sigma)_{n\alpha} (G_0^+ \Sigma)_{\alpha i}] [(G_0^- \Sigma)_{m\beta} (G_0^- \Sigma)_{\beta k}] \end{aligned} \quad (\text{D12})$$

$$+ g^2 [(G_0^+ \Sigma)_{n\alpha} (G_0^- \Sigma)_{m\beta}] [(G_0^+ \Sigma)_{\alpha i} (G_0^- \Sigma)_{\beta k}] \quad (\text{D13})$$

$$+ g^2 [(G_0^+ \Sigma)_{n\alpha} (G_0^- \Sigma)_{\beta k}] [(G_0^+ \Sigma)_{\alpha i} (G_0^- \Sigma)_{m\beta}] \quad (\text{D14})$$

+ higher orders.

Line (D12) represents a self-energy contribution. The total effect arising from summing all diagrams in this class can be accounted by the replacement of naked propagators by the renormalized ones, i.e. $G_0^\pm \rightarrow \bar{G}^\pm$ via $\epsilon \rightarrow \epsilon + \eta$. The diagram class given by the complete geometric series

$$\begin{aligned} (1 - t)_{rr'|nm;ik}^{-1} &= \delta_{rr'} \delta_{ni} \delta_{mk} + g [(G_0^+ \Sigma)_{ni} (G_0^- \Sigma)_{mk}]_{rr'} \\ &+ g^2 [(G_0^+ \Sigma)_{n\alpha} (G_0^- \Sigma)_{m\beta}] [(G_0^+ \Sigma)_{\alpha i} (G_0^- \Sigma)_{\beta k}]_{rr'} + \dots \\ &= [1 - g(\bar{G}^+ \Sigma)(\bar{G}^- \Sigma)]_{rr'|nm;ik}^{-1}, \end{aligned} \quad (\text{D15})$$

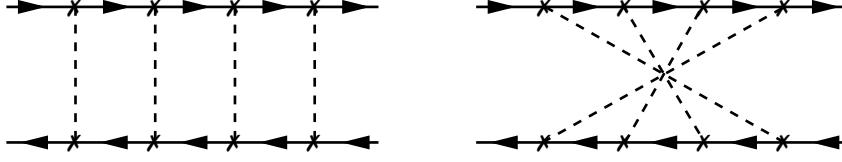


FIG. 1: A generic diagram from the ladder (left) and from the maximally crossed (right) class.

is called the ladder class. The corresponding diagrammatic representation is shown in Fig. 1 on the left. For manipulations in Line (D14) we note that $(\bar{G}^-\Sigma)_{ab} = (\bar{G}^-\Sigma)_{ba}^T$, where, the transposition operator T applies to all degrees of freedom, i.e. to the spatial ones as well. This class of diagrams is called the maximally crossed class and is shown in Fig. 1 on the right. This series is incomplete with missing zero and first order terms. Introducing them we can perform the summation of this diagram class, obtaining

$$\begin{aligned}
 (1 - \tau)_{rr'|nk;im}^{-1} &= \delta_{rr'}\delta_{ni}\delta_{km} + g [(\bar{G}^+\Sigma)_{ni}(\bar{G}^-\Sigma)_{km}^T]_{rr'} \\
 &+ g^2 [[(\bar{G}^+\Sigma)_{n\alpha}(\bar{G}^-\Sigma)_{k\beta}^T][(\bar{G}^+\Sigma)_{\alpha i}(\bar{G}^-\Sigma)_{\beta m}^T]]_{rr'} + \dots \\
 &= [1 - g(\bar{G}^+\Sigma)(\bar{G}^-\Sigma)^T]_{rr'|nk;im}^{-1}.
 \end{aligned} \tag{D16}$$

Neglecting higher order diagrams we then obtain

$$\begin{aligned}
 \langle G_{nj}^+ G_{ml}^- \rangle &\sim \left([1 - g(\bar{G}^+\Sigma)(\bar{G}^-\Sigma)]_{nm;ik}^{-1} + [1 - g(\bar{G}^+\Sigma)(\bar{G}^-\Sigma)^T]_{nk;im}^{-1} \right. \\
 &\quad \left. - [1 + g(\bar{G}^+\Sigma)(\bar{G}^-\Sigma)^T]_{nk;im} \right) \bar{G}_{ij}^+ \bar{G}_{kl}^-,
 \end{aligned} \tag{D17}$$

where first term in the parenthesis denote the ladder channel matrix, second term the maximally crossed channel matrix and the remaining terms are introduced in order to avoid the double counting. Addressing Eq. (31) it is clear, that none of the elements from the second line can develop a ϵ^{-2} singularity and thus disappear from the conductivity in the dc limit. Therefore we ignore them in further analysis.

-
- ¹ E. Abrahams, P. W. Anderson, D. C. Licciardello, and T. V. Ramakrishnan, Phys. Rev. Lett. **42**, 673 (1979).
 - ² L. G. Gor'kov, A. I. Larkin, and D. E. Khmel'nitskii, Pis'ma Zh. Eksp. Teor. Fiz. **30**, 248 (1979) [JETP Lett. **30**, 228 (1979)].
 - ³ S. Hikami, A. Larkin, and Y. Nagaoka, Prog. Theor. Phys. **63**, 707 (1980).
 - ⁴ D. Vollhardt and P. Wölfle, Phys. Rev. B **22**, 4666 (1980).
 - ⁵ Y. Hanein, U. Meirav, D. Shahar, C.C. Li, D.C. Tsui, and H. Shtrikman Phys. Rev. Lett. **80**, 1288 (1998).
 - ⁶ K. S. Novoselov, A. K. Geim, S. V. Morozov, D. Jiang, M. I. Katsnelson, I. V. Grigorieva, S. V. Dubonos, and A. A. Firsov, Nature **438**, 197 (2005).
 - ⁷ Y.-W. Tan, Y. Zhang, K. Bolotin, Y. Zhao, S. Adam, E. H. Hwang, S. Das Sarma, H. L. Stormer, and P. Kim, Phys. Rev. Lett. **99**, 246803 (2007).
 - ⁸ D. C. Elias, R. R. Nair, T. M. G. Mohiuddin, S. V. Morozov, P. Blake, M. P. Halsall, A. C. Ferrari, D. W. Boukhvalov, M. I. Katsnelson, A. K. Geim, and K. S. Novoselov, Science **323**, 610 (2009).
 - ⁹ M. J. Allen, V. C. Tung, and R. B. Kaner, Chem. Rev. **110**, 132 (2010).
 - ¹⁰ L. Chen, Ch.-Ch. Liu, B. Feng, X. He, P. Cheng, Z. Ding, Sh. Meng, Y. Yao, and K. Wu, Phys. Rev. Lett. **109**, 056804 (2012).
 - ¹¹ M. Z. Hasan and C. L. Mele, Rev. Mod. Phys. **82**, 3045 (2010).
 - ¹² X.-L. Qi and S.-C. Zhang, Rev. Mod. Phys. **83**, 1057 (2011).
 - ¹³ N. H. Shon and T. Ando, J. Phys. Soc. Jap. **67**, 2421 (1998).
 - ¹⁴ T. Ando, Y. Zheng and H. Suzuura, J. Phys. Soc. Japan **71**, 1318 (2002); H. Suzuura and T. Ando, Phys. Rev. Lett. **89**, 266603 (2002).
 - ¹⁵ E. McCann, K. Kechedzhi, Vladimir I. Fal'ko, H. Suzuura, T. Ando, and B. L. Altshuler Phys. Rev. Lett. **97**, 146805 (2006).
 - ¹⁶ D.V. Khveshchenko, Phys. Rev. Lett. **97**, 036802 (2006).
 - ¹⁷ B. L. Altshuler, A. G. Aronov, A. I. Larkin, and D. E. Khmel'nitskii, Th. Eksp. Teor. Fiz. **81**, 768 (1981) [Sov. Phys. JETP **54**, 411 (1981)].

- ¹⁸ G. Tkachov and E.M. Hankiewicz, Phys. Rev. B **84**, 035444 (2011).
- ¹⁹ D. Schmeltzer and A. Saxena, Phys. Rev. B **88**, 035140 (2013).
- ²⁰ B. L. Altshuler and B. D. Simons in E. Akkermans, G. Montambaux, J.-L. Pichard, and J. Zinn-Justin, *Mesoscopic quantum physics, Les Houches 1994*, North Holland, Amsterdam (1995).
- ²¹ K. Efetov, *Supersymmetry in disorder and chaos*, Cambridge University Press, Cambridge UK (1997).
- ²² L. S. Levitov and A. V. Shytov, *Green's functions. Theory and practice, in Russian*, <http://www.mit.edu/~levitov/book/>.
- ²³ F. J. Wegner, Phys. Rev. B **19**, 783 (1979).
- ²⁴ A. J. McKane and M. Stone, Ann. Phys. **131**, 36 (1981).
- ²⁵ E. Fradkin, Phys. Rev. **33**, 3257 (1986); *ibid* 3263 (1986).
- ²⁶ K. Ziegler, Phys. Rev. B **55**, 10661 (1997); K. Ziegler and G. Jug, Z. Phys. B **104**, 5 (1997); K. Ziegler, Phys. Rev. Lett. **80**, 3113 (1998).
- ²⁷ F. Wegner, Z. Physik B **35**, 207 (1979).
- ²⁸ L. Schäfer and F. Wegner, Z. Physik B **38**, 113 (1980).
- ²⁹ S. Hikami, Phys. Rev. B **24**, 2671 (1981).
- ³⁰ K. Ziegler, Phys. Rev. Lett. **102**, 126802 (2009); Phys. Rev. B **79**, 195424 (2009).
- ³¹ K. Ziegler, J. Phys. A: Math. Theor. **45**, 335001 (2012).
- ³² K. Ziegler and A. Sinner, Phys. E **71**, 14 (2015).
- ³³ A. Sinner and K. Ziegler, J. Phys.: Condens. Matter *in press*, arXiv:1602.02786 (2016).
- ³⁴ A. Sinner and K. Ziegler, Phys. Rev. B **84**, 233401 (2011).
- ³⁵ A. Sinner and K. Ziegler, Phys. Rev. B **89**, 024201 (2014).
- ³⁶ A. Sinner, A. Sedrakyan, and K. Ziegler, Phys. Rev. B **83**, 155115 (2011).
- ³⁷ K. Ziegler and A. Sinner, Phys. Rev. B **81**, 241404(R) (2010).
- ³⁸ A. Sinner and K. Ziegler, Phys. Rev. B **90**, 174207 (2014).
- ³⁹ A. Sinner and K. Ziegler, Phys. Rev. B **86**, 155450 (2012).
- ⁴⁰ A. W. W. Ludwig, M. P. A. Fisher, R. Shankar, and G. Grinstein, Phys. Rev. B **50**, 7526 (1994).
- ⁴¹ P. K. Wallace, Phys. Rev. **71**, 622 (1947).
- ⁴² G. W. Semenoff, Phys. Rev. Lett. **53**, 2449 (1984).
- ⁴³ A. A. Burkov, J. Phys.: Condens. Matter **27**, 113201 (2015).
- ⁴⁴ K. Huang, *Statistical mechanics*, Wiley Inc. (1963).
- ⁴⁵ M. R. Zirnbauer, J. Math. Phys. **37**, 4986 (1996).
- ⁴⁶ A. Altland and M. Zirnbauer, Phys. Rev. B **55**, 1142 (1997).
- ⁴⁷ D. Bernard and A. LeClair, J. Phys. A: Math. Gen. **35**, 2555 (2002).
- ⁴⁸ D. Bernard, E.-A. Kim, and A. LeClair, Phys. Rev. B **86**, 205116 (2012).